sustainability

MDPI

Article

Sustainable Treatment of Fisheries Wastewater Using *Azadirachta indica* Leaf Biocoagulant: Optimization of Chemical Oxygen Demand and Total Suspended Solid Removal

Muhammad Fauzul Imron [1,2,3,*], Rikky Ramadhan Mustofa [1], Wahid Dianbudiyanto [1], Eko Prasetyo Kuncoro [1], Suriya Vathi Subramanian [4] and Setyo Budi Kurniawan [5]

[1] Study Program of Environmental Engineering, Department of Biology, Faculty of Science and Technology, Universitas Airlangga, Kampus C UNAIR, Jalan Mulyorejo, Surabaya 60115, Indonesia; rikkyramadhanm@gmail.com (R.R.M.); dian.budiyanto@fst.unair.ac.id (W.D.); eko-p-k@fst.unair.ac.id (E.P.K.)
[2] Research Group of Sustainable Environmental Systems and Infrastructure (SUSTAIN), Faculty of Science and Technology, Universitas Airlangga, Kampus C UNAIR, Jalan Mulyorejo, Surabaya 60115, Indonesia
[3] Department of Water Management, Faculty of Civil Engineering and Geosciences, Delft University of Technology, Stevinweg 1, 2628 CN Delft, The Netherlands
[4] Department of Chemical and Process Engineering, Faculty of Engineering and Built Environment, Universiti Kebangsaan Malaysia, Bangi 43600, Selangor, Malaysia; p141373@siswa.ukm.edu.my
[5] Research Center for Environment and Clean Technologies, National Research and Innovation Agency (BRIN), Jakarta Pusat 10340, Indonesia; setyo.budi.kurniawan@brin.go.id
* Correspondence: fauzul.imron@fst.unair.ac.id or m.f.imron@tudelft.nl

Abstract

Fisheries wastewater contains high levels of suspended solids and organic matter, posing significant environmental risks and necessitating effective and sustainable treatment approaches. This study aims to determine the characteristics of the neem (*Azadirachta indica*) leaf biocoagulant, assess the interactions among research variables, and optimize its use to reduce total suspended solids (TSS) and chemical oxygen demand (COD) levels in fisheries wastewater. The method used is response surface methodology (RSM), specifically the Box–Behnken Design (BBD), which involves three variables (biocoagulant concentration, fast stirring speed, and sedimentation time) and two responses (TSS and COD removal). Characterization results (Fourier Transform Infrared Spectroscopy (FTIR), Scanning Electron Microscopy (SEM), X-ray Diffraction (XRD), and zeta potential) indicated that the biocoagulant contains functional groups such as hydroxyl, carboxyl, and amine, contributing to coagulation–flocculation through adsorption and polymer bridging mechanisms. Statistical analysis confirmed that the developed quadratic models were significant (p-value < 0.05), with high F-values, non-significant lack of fit, and strong coefficients of determination (R^2 = 0.9111 for TSS and 0.9419 for COD), along with low coefficients of variation (CV < 5%), indicating good model reliability. Although the model generally has a significant effect on the response, the fast stirring speed does not, while the other two factors do. The optimal conditions (based on desirability) were determined to be a biocoagulant concentration of 79.8 mg/L, a fast stirring speed of 100 rpm, and a sedimentation time of 27.5 min. Under these conditions, TSS and COD removals of 88.72% and 79.98%, respectively, were achieved. These findings demonstrate the potential of neem leaf biocoagulant as a sustainable, environmentally friendly alternative to conventional chemical coagulation, supporting cleaner production in aquaculture systems.

Keywords: aquaculture effluent; biocoagulant; coagulation–flocculation; green technology; neem; sustainable aquaculture; wastewater treatment

Academic Editor: Yong Xiao

Received: 6 April 2026
Revised: 24 April 2026
Accepted: 24 April 2026
Published: 1 May 2026

1. Introduction

Fisheries cultivation is a rapidly growing sector that contributes significantly to the global economy, but it also generates substantial volumes of wastewater due to intensive water use [1]. This wastewater is characterized by high concentrations of organic matter and nutrients, including chemical oxygen demand (COD), total suspended solids (TSS), nitrogen, and phosphorus, which can lead to environmental problems such as eutrophication and ecosystem disruption [2]. Previous studies have shown the characteristics of fisheries wastewater, including pH 6.5–8.2; dissolved oxygen (DO) 4–6.5 mg/L; TSS 70–2136 mg/L; COD 20.5–2394 mg/L; ammonia 0.18–9.45 mg/L; and phosphate up to 32.5 mg/L [3]. High levels of organic matter and nutrients can adversely affect water bodies, leading to eutrophication [4,5]. Other negative impacts include disruption of the aquatic ecosystem due to pathogenic bacteria, harmful plankton, and increased levels of toxic compounds [6,7]. Therefore, effective and sustainable wastewater treatment strategies are required to mitigate these impacts [8].

Among the available treatment methods, coagulation–flocculation is widely used for its effectiveness, simplicity, and cost-effectiveness in removing suspended solids and organic pollutants [9,10]. Conventional coagulants, such as alum and polyaluminium chloride (PAC), have demonstrated high removal efficiencies [11,12]; however, their long-term use raises environmental and health concerns. These include the generation of non-biodegradable sludge dominated by stable metal hydroxides [13] and the potential risks associated with residual metal exposure, such as the risk of developing Alzheimer's disease [14,15]. As a result, the development of natural coagulants (biocoagulants) has gained increasing attention as a more sustainable alternative [16].

Biocoagulants derived from animal sources [17], plant sources [18], and microorganisms [19] offer advantages such as biodegradability, low toxicity, and environmental compatibility [20]. Among them, plant-based biocoagulants are particularly attractive due to their abundance and renewability [21]. Plant-based biocoagulants that have been developed in several studies include banana peel (*Musa paradisica*)-based biocoagulants with the ability to reduce turbidity by 98.14% [22], castor bean-based biocoagulants (*Ricinus communis*) with the ability to reduce COD by 80% and TDS by 75% [23], and moringa leaf-based biocoagulant (*Moringa oleifera*) with the ability to reduce turbidity by 96% and COD by 88% [24]. Neem leaves (*Azadirachta indica*), in particular, have shown promising performance, achieving significant reductions in TSS by 84% and COD by 86% [25]. The use of neem leaves is currently being developed, especially as a biocoagulant. Several studies have identified that neem leaves can reduce TSS levels by 81–84% [25,26] and reduce COD levels by 49–86% [20,25]. The performance of the neem leaf biocoagulant can be further improved through optimization, with Response Surface Methodology (RSM) among the commonly used models [27–29].

Several biocoagulant studies that have successfully determined optimal conditions using the RSM method include those by Ezemagu et al. [30] and Thirugnanasambandham and Karri [20]. Ezemagu et al. [30] studied the performance of *Tympanotonos fuscatus* shell-based biocoagulants, which can reduce turbidity by 83% in oil industry produced water wastewater under optimum conditions, namely using a dose of 1 g/L, a time of 16.5 min, and a temperature of 45 °C [30]. Thirugnanasambandham and Karri [20] studied a neem leaf-based biocoagulant that can reduce turbidity levels by 73%, color by 69%, and COD by 48% under optimum conditions using a dose of 4 g/L, a stirring speed of 30 rpm, and a sedimentation time of 55 min [20].

The development of neem leaf-based biocoagulant has good potential for the future of wastewater treatment. Research on its use as a biocoagulant in fisheries wastewater is still limited [26]. Therefore, this study aims to optimize the use of neem leaf-based

biocoagulant for the removal of COD and TSS from fisheries wastewater using RSM with a Box–Behnken Design. In addition, this study uses a fast stirring speed, a variable previously studied for biocoagulants but not applied to neem leaf biocoagulants. This work contributes to the development of sustainable and environmentally friendly wastewater treatment approaches for the aquaculture sector.

2. Materials and Methods

2.1. Wastewater Collection

This study comprises a series of processes across several research sites. Sampling of fishery wastewater was carried out at the Pokdakan Sedangmijen Makmur location (catfish farming pond), Krian District, Sidoarjo Regency, with location coordinates of 7°25′48.2″ S and 112°35′02.9″ E. Sampling of fishery wastewater was carried out by referring to the procedures stated in SNI 6989.59:2008 [31] Section 59 on Wastewater Sampling Methods. Sampling was carried out in industries that lacked a wastewater treatment plant, a batch process, an equalization tank, or fluctuating wastewater quality. With these characteristics, sampling was conducted briefly in the channel before entering the water body receiving the wastewater. Wastewater sampling was conducted as a grab sample collected from a single point. Sampling was performed during the rainy season; however, it was carried out on a non-rainy day to minimize dilution effects. The ambient temperature during sampling was approximately 30–32 °C. The sampling tool was a simple polyethylene plastic bucket equipped with a rope. The sample water was then placed in a polyethylene jerrycan capable of holding 20 L of wastewater, free from contaminants, and able to be closed tightly without breaking or interacting with the sample. The sample container had previously undergone a preparation step, consisting of washing the container and lid with phosphate-free detergent and rinsing them with clean water. After that, the container was washed with 1:1 hydrochloric acid (HCl), then rinsed with analyte-free water three times.

2.2. Leaves Collection and Biocoagulant Preparation

Neem (*Azadirachta indica*) leaves were obtained from medicinal plant cultivation in Jember Regency. Biocoagulant preparation, experimental setup, and wastewater sample analysis were carried out at the Ecology and Environment Laboratory and Laboratory 303 Pertamina, Faculty of Science and Technology, Airlangga University. Preparation of neem leaves was carried out through a series of procedures, starting with washing the neem leaves using distilled water. The neem leaves were then dried using an oven at 40 °C for 72 h. The dried neem leaves were ground using a blender. The ground material was sieved through a 100-mesh sieve to obtain a uniform powder with a particle size less than 150 µm [20]. The powder was stored as a biocoagulant used in this study.

The biocoagulant was used in crude powder form, without chemical purification, to reflect a practical, economically feasible application in wastewater treatment. This approach is consistent with most plant-based coagulation studies, in which process performance, rather than isolated compound activity, is the primary objective [32,33].

2.3. Characterization of Biocoagulant

2.3.1. Functional Group Analysis

FTIR is used to identify organic, inorganic, and polymer materials by scanning samples with infrared light [27]. FTIR also analyzes the concentration and type of functional groups to identify the compounds or active groups in biocoagulants that facilitate coagulation and flocculation. The FTIR spectrum of neem leaf biocoagulant powder was recorded to determine the chemical characteristics, and the FTIR spectrum was measured in the range of 400–4000 cm^{-1} [20]. FTIR analysis was performed on neem leaf biocoagulants

to identify functional groups involved in the coagulation process using the IR Affinity-1 model (Shimadzu, Kyoto, Japan) [34].

2.3.2. Surface Morphology Analysis

Scanning Electron Microscopy (SEM) analysis was conducted to examine the surface morphology and microstructure of the neem leaf biocoagulant before and after the coagulation–flocculation process [35]. The analysis was performed using a Quanta 250 FEI scanning electron microscope (FEI, Hillsboro, OR, USA). Samples were prepared by dispersing the dried material onto double-sided carbon tape mounted on an aluminum stub, then sputter-coating it with a thin layer of gold to enhance conductivity. Imaging was carried out under high-vacuum conditions at an accelerating voltage of 20 kV. Micrographs were obtained at a magnification of 10,000× to observe surface characteristics, including roughness, fragmentation, and floc formation [36].

2.3.3. Crystallographic Analysis

X-Ray Diffraction (XRD) is a technique commonly used to characterize the structure and composition of a material [37]. In general, XRD can identify the phase of the material, namely amorphous, crystalline, or semi-crystalline, and conclude the compounds contained therein [38]. XRD analysis was performed using an X'Pert MPD diffractometer (Malvern Instruments, Malvern, UK) equipped with Cu Kα radiation (λ = 1.5406 Å). The instrument was operated at a voltage of 40 kV and a current of 30 mA. Data were collected over a 2θ range of 10.0° to 89.98° with a step size of 0.017° and a scan step time of 10.15 s in continuous-scanning mode. A fixed divergence slit of 1° was used, with a receiving slit size of 12.75 mm. Measurements were conducted without a monochromator and without sample spinning.

2.3.4. Zeta Potential Analysis

Zeta potential analysis was conducted to determine the surface charge characteristics of the neem leaf biocoagulant and the wastewater. Measurements were performed using a ZetaSizer Nano ZS90 (Malvern Instruments, Malvern, UK) equipped with a DTS1061 capillary cell. The biocoagulant sample was prepared as an aqueous extract and analyzed together with the wastewater sample. All measurements were carried out at a controlled temperature of 25 °C [2]. Before analysis, samples were gently mixed to ensure homogeneity and introduced into the capillary cell without air bubbles. The zeta potential values were obtained based on electrophoretic mobility measurements using the Smoluchowski model. Each measurement was performed in triplicate, and the average values were reported.

2.4. Jar Test Experiment

The jar test is used to determine the ability of coagulants to reduce pollutant levels [39,40]. The jar test is carried out in accordance with Indonesian National Standard 19-6449-2000 [41], which specifies the coagulation–flocculation testing method by the jar method. The jar test is carried out by preparing 1000 mL of fishery wastewater samples in 18 beakers. A biocoagulant was added at a specific concentration based on the experimental design (Section 2.5). The jar test begins by placing the beaker containing the sample and biocoagulant on the jar test stirring unit, and fast stirring is started for 1 min, with stirring speed varying according to the level code for each experiment. After fast stirring, slow stirring is performed for 30 min at 30 rpm [42]. Sedimentation, the final step of the jar test, is performed by leaving the jar for a predetermined time.

2.5. Optimization Design

The range and level of factors (independent variables) are determined by their coding, which is divided into three levels: −1, 0, and +1. Coding is carried out using a minimum of three factors, each with a specified range of values derived from literature studies [30,43]. Factor-level coding was applied to three independent variables: biocoagulant concentration (A), fast stirring speed (B), and sedimentation time (C). The two responses observed in this study were decreases in TSS (%) and COD (%). This study also included two types of controls: negative controls (without coagulants) and positive controls (with commercial alum coagulants at 17%). Coding with three factors at three levels yielded 17 experiments (Table 1). A total of 5 central points were used to estimate experimental errors.

Table 1. Experimental design based on BBD with 5 central points.

Run Order	A	B	C	Response 1	Response 2
	Biocoagulant Concentration	Fast Stirring Speed	Sedimentation Time		
	(mg/L)	(rpm)	(min)		
1	50	150	20	TSS removal (%)	COD removal (%)
2	50	100	10		
3	80	150	30		
4	80	150	10		
5	50	150	20		
6	20	150	30		
7	50	200	30		
8	50	150	20		
9	80	100	20		
10	20	100	20		
11	50	150	20		
12	50	100	30		
13	20	150	10		
14	50	150	20		
15	80	200	20		
16	20	200	20		
17	50	200	10		
Control −	0	200	30		
Control +	80	200	30		

Confirmation experiments were conducted on variables estimated to yield the optimum response. Confirmation experiments were conducted to validate the results of the optimization process. Optimum conditions are determined using the desirability value approach. Desirability is a value obtained from a mathematical function approach. The desirability function approach is implemented by determining the level of response priority (constraints) within a specified range of values, based on the results of qualitative and quantitative analyses. The optimization objective can also be set to maximize, minimize, or achieve a specific target response value [44,45]. The resulting data were compared with the estimated values generated by the optimization process to assess whether the optimization results could be confirmed [44,45].

2.6. Parameter Analysis

The Total Suspended Solids (TSS) parameter test follows Standard Method Protocol No. 2540, the gravimetric method of testing total suspended solids [46]. The Chemical Oxygen Demand (COD) parameter test is described in Standard Method Protocol No. 5220, Method of Testing Chemical Oxygen Demand (COD) with closed reflux spectrophotometry [47]. The efficiency of TSS and COD removal is calculated based on TSS and COD levels before and after the jar test. All analyses were conducted in triplicate.

2.7. Statistical Analysis

Statistical analysis was conducted using the RSM-BBD. The statistical analyses conducted included regression analysis and model testing, model coefficient analysis, analysis of interactions between factors on the dependent variable, and optimization using the desirability function. The statistical analysis instrument used was Design-Expert 13.0.5 (Stat-Ease Inc., Minneapolis, MN, USA).

3. Results and Discussions

3.1. Initial Characteristics of Fishery Wastewater

A preliminary test was conducted as a pollutant parameter level test to determine the initial characteristics of the wastewater used in the study, as presented in Table 2.

Table 2. Initial characteristics of wastewater.

Parameter	Unit	Concentration/Value	Method
pH	-	8.63	pH meter
Turbidity	NTU	320	Turbidimetry
Color	Unit PtCo	1488.45	Spectrophotometry
TSS	mg/L	177.30	Gravimetry
DO	mg/L O_2	1.60	Iodimetry
COD	mg/L O_2	585.66	Reflux
BOD	mg/L O_2	260	Winkler
Nitrite	mg/L NO_2N	0.08	Spectrophotometry
Nitrate	mg/L NO_3-N	0.26	Spectrophotometry
Ammonia	mg/L NH_3-N	1.21	Spectrophotometry
Total N	mg/L NH_3-N	6.63	Kjeldahl
Total P	mg/L PO_4-P	57.81	Spectrophotometry

Based on the results of the initial wastewater characteristic test presented in Table 2, the fishery wastewater contains relatively high levels of TSS and organic matter (COD), namely 177.3 mg/L and 583.35 mg/L, respectively. Solids and organic matter in fishery wastewater are caused by the presence of leftover feed, feces, and fish excretion waste [48,49]. The nutrient content in fishery wastewater is due to the use of fertilizers to support fish productivity [50,51]. High levels of solids, organic matter, and nutrients in fishery wastewater can negatively impact the quality of receiving rivers, thereby causing eutrophication [4]. Thus, research on the use of neem leaf biocoagulant was conducted as an alternative for processing fishery wastewater to avoid causing water pollution.

3.2. Characteristics of Biocoagulant

3.2.1. Functional Groups

The FTIR spectra of the neem leaf biocoagulant are presented in Figure 1 and summarized in Table 3.

Table 3. Interpretation of FTIR spectra for neem leaf biocoagulant.

Wavenumber (cm^{-1})	Bound	Vibration Type	Intensity	Vibration Mode	Reference (cm^{-1})	Representative Compounds
3287.22	O-H	Broad	Strong	Stretch	~3200–3550	Polysaccharides, phenolics
2920.75 and 2846.78	NH_2	Sharp	Strong	Stretch	~3300–3500	Proteins, amino acids
1730.55	C=O	Sharp	Medium	Stretch	~1710–1780	Flavonoids, tannins
1602.79	NH_2	Sharp	Strong	Scissor	~1601	Proteins
1239.67	C-O	Sharp	Strong	Stretch	~1200	Polysaccharides
1038	C-N	Sharp	Strong	Stretch	~650–1550	Proteins

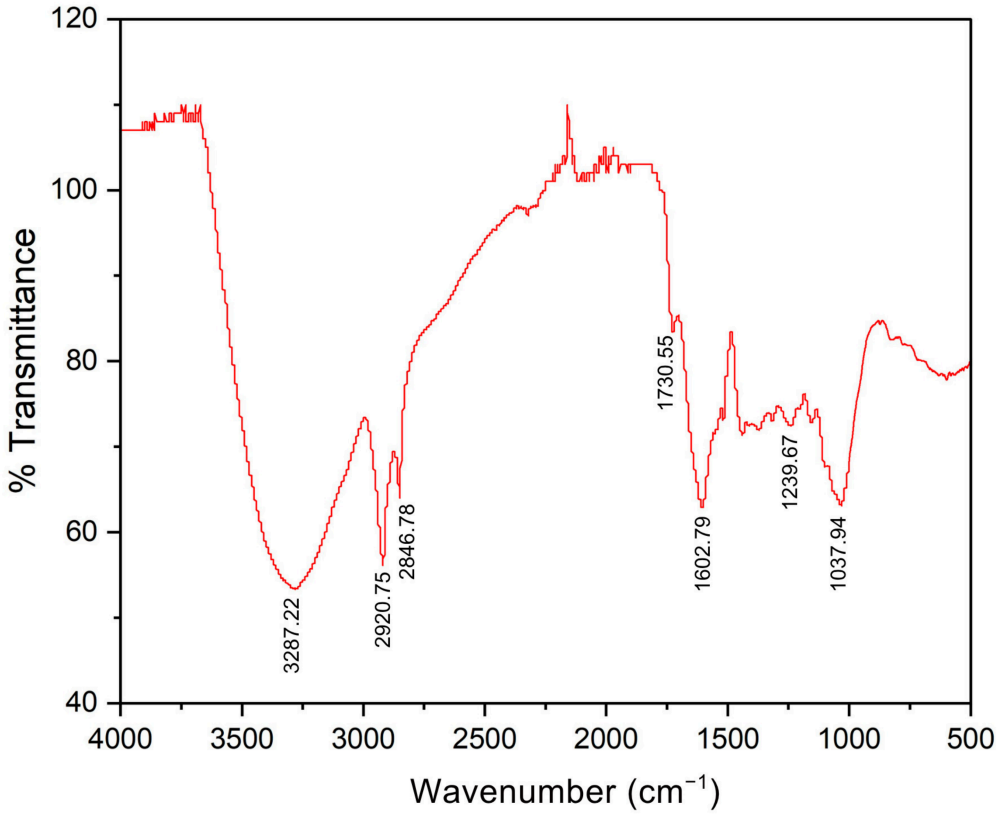

Figure 1. FTIR spectra of neem leaf biocoagulant.

The FTIR spectrum of neem powder shown in Figure 1 reveals a distinct band indicating the presence of a specific functional group, supporting the potential biocoagulant function of neem leaves. The distinctive broad band centered at 3287.22 cm^{-1} corresponds to the O-H stretching. This validates the presence of hydroxyl groups within polysaccharides or phenolic groups in neem leaves that facilitate coagulation via hydrogen bonding, bridging, and charge neutralization [52]. The presence of C=O stretching vibrations at the peak of 1730.55 cm^{-1} validates the presence of carboxyl groups in flavonoids, tannins, and phenolics of the neem leaves group, which commonly involve an absorption mechanism [53,54]. Furthermore, the sharp peaks at 2930.75 cm^{-1} and 2846.75 cm^{-1} indicated the presence of N-H stretching vibrations in primary amines, which is further supported by the N-H scissoring vibration at 1602.79 cm^{-1}. Additional sharp peaks at 1239.67 cm^{-1} and 1038 cm^{-1} indicated the presence of C-O and C-N stretching. The presence of a C-N bond suggests the existence of nitrogen-containing compounds that can be found in proteins. The result obtained was consistent with previous studies, which reported that FTIR analysis of neem leaves revealed hydroxyl, carboxyl, and amine groups [2,55,56]. According to Kurniawan et al. [57], the detected functional groups in this biocoagulant, such as hydroxyl, carboxyl, amine, and protein, contribute to excellent efficiency in the coagulation process for pollutants in fishery wastewater. Although the active coagulating species were not isolated, the FTIR and zeta potential results indicate that proteinaceous and polyphenolic functional groups are the dominant contributors to coagulation [58,59]. Similar structure–performance correlations have been widely used to explain the activity of crude plant biocoagulants in real wastewater matrices [32,33,60].

3.2.2. Surface Morphology

Figure 2 shows the surface morphological characteristics of Neem powder before and after the biocoagulant preparation steps. This SEM micrograph was captured at a

magnification of 10,000× and an excitation voltage of 20 kV. The neem leaf surface, as depicted in Figure 2a, shows irregular particles with fragmented lamellae. However, after the mechanical preparation step involving drying and sieving through a 100-mesh screen, the neem powder displays a more fragmented, rough, and flaky surface (Figure 2b). This implies that the neem leaves were ground perfectly to produce finer particles. This change in surface morphology can enhance the specific surface area, promoting greater contact between the biocoagulant's active functional groups and pollutants [61].

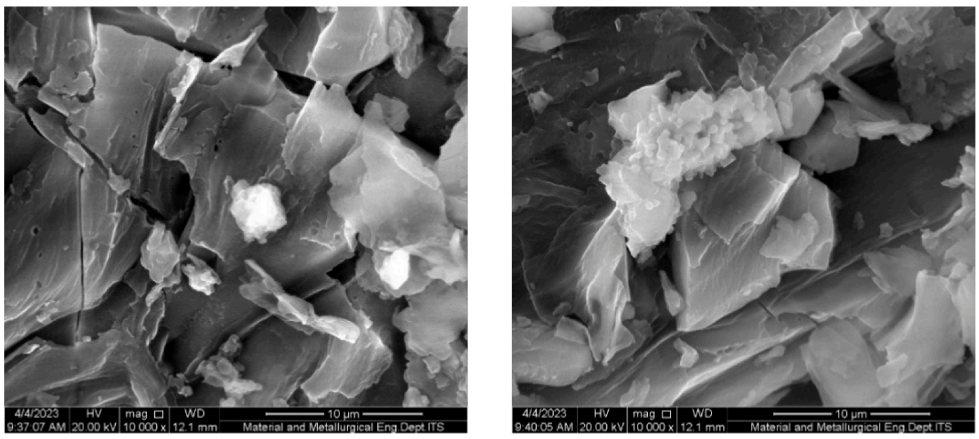

(**a**) (**b**)

Figure 2. SEM images of biocoagulants (**a**) Neem leaves before biocoagulant preparation and (**b**) Neem powder as biocoagulant.

3.2.3. Crystallographic Structure

The results of the XRD test of the neem leaf biocoagulant are presented in Figure 3, which plots the X-axis (2θ angle) against the Y-axis (peak intensity). Furthermore, a literature review was conducted to identify the compounds present in the neem leaf biocoagulant.

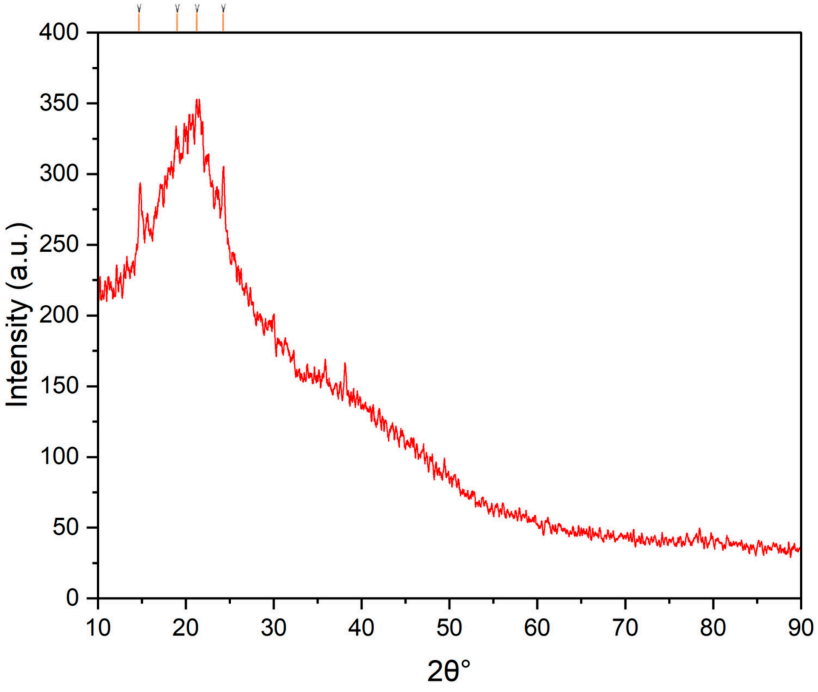

Figure 3. XRD pattern of neem powder before treatment. The XRD pattern was smoothed using a Savitzky–Golay filter (window size = 21 points, polynomial order = 3) to improve visualization while preserving peak characteristics.

Based on Figure 3, four main peaks were obtained, which were located at the angles of 2θ 14.80°, 19.12°, 21.40°, and 24.32°. The peak at an angle of 2θ 14.80° is the peak with the lowest intensity when compared to other main peaks. The broad peak in the 20° to 25° range suggests a poorly defined mineral phase. A peak between 15° and 40° indicates the presence of organic compounds. Specific 20° peaks indicate that the material is amorphous and contains significant amounts of protein structural components. This outcome confirms the presence of an amorphous structure and aligns with the previous finding, which also reported a similar result for neem powder [62]. This indicates that the atoms are randomly organized, without long-range order or repetition.

3.2.4. Zeta Potential

The results of the zeta potential test of neem leaf biocoagulant and fishery wastewater samples are presented in Table 4. Table 4 shows that the neem leaf biocoagulant and the fishery wastewater sample water have negative charges of −18.21 mV and −19.40 mV, respectively. This result was consistent with a previous study reporting an average zeta potential of −22.83 ± 0.62 mV for water extracted from neem leaves [2]. The negatively charged neem leaf biocoagulant indicates the presence of protein compounds, as negative charges dominate its surface. The surface charge of protein compounds is greatly influenced by the level of acidity (pH). When the pH is above the isoelectric point, the protein will have a negative surface charge [63,64].

Table 4. Measured zeta potential.

Sample	Value	Unit
Neem leaf biocoagulant	−18.21	mV
Fishery wastewater	−19.40	mV

The removal of TSS and COD by neem leaf biocoagulant can be explained through a combination of physicochemical mechanisms. FTIR analysis revealed the presence of hydroxyl, carboxyl, and amine functional groups, which facilitate adsorption and polymer bridging between particles. The SEM images showed a rough, heterogeneous surface morphology, thereby enhancing contact between the biocoagulant and suspended particles. XRD analysis confirmed the predominantly amorphous structure of the material, which is favorable for adsorption due to the absence of rigid crystalline order. Furthermore, the negative zeta potentials of both the biocoagulant and the wastewater suggest that coagulation occurs primarily through adsorption and interparticle bridging [2,65,66], while charge neutralization may be enhanced under modified pH conditions [3].

Previous research identified the presence of negatively charged protein compounds in *Musa acuminata*-based biocoagulants [67]. In the previous literature, the acidity level was adjusted to pH < 4.8 by the addition of 0.1 N of HNO_3, resulting in the protonation of several functional groups, such as amino and carboxyl groups. These results enhance the ability to remove colloidal particles by increasing positive charge and density and by providing a strong electrostatic force on negatively charged colloidal particles. Similar conditioning could be explored in future studies to modify the surface charge of neem leaf biocoagulants, for example, by adjusting the pH to induce protonation of functional groups. Such an approach may enhance charge neutralization and improve the removal efficiency of pollutant particles; however, this was not investigated in the present study.

3.3. Optimization of Fishery Wastewater Treatment

TSS and COD removal percentages based on the BBD run order are presented in Table 5. Based on Table 5, the TSS and COD removal responses varied across experiments.

The highest TSS removal, 85.71%, was observed in experiment 7, with a biocoagulant concentration of 50 mg/L, a stirring speed of 200 rpm, and a sedimentation time of 30 min. The lowest TSS removal was observed in experiment 17 (63.90%), with a biocoagulant concentration of 50 mg/L, a stirring speed of 200 rpm, and a sedimentation time of 10 min. Meanwhile, the highest COD removal was observed in experiment 12, at 73.47%, with a biocoagulant concentration of 50 mg/L, a stirring speed of 100 rpm, and a sedimentation time of 30 min. The lowest COD removal was observed in experiment 13, at 54.14%, with a concentration of 20 mg/L, a stirring speed of 150 rpm, and a sedimentation time of 10 min. Compared with the negative control, the neem leaf biocoagulant reduced TSS and COD levels more effectively, with the lowest response showing a significantly higher percentage removal. However, compared with the positive control, alum was more effective at reducing TSS and COD, with the smallest differences of 3.01% for TSS and 19.13% for COD. Although alum exhibited slightly higher removal efficiencies, the use of neem leaf biocoagulant is justified by its environmental advantages, including biodegradability, lower toxicity, and reduced risk of residual metal accumulation. In addition, the use of plant-based materials supports sustainable and low-cost wastewater treatment, making it a promising alternative to conventional chemical coagulants.

Table 5. Experimental run results.

Run Order	A	B	C	Response 1	Response 2
	Biocoagulant Concentration	Fast Stirring Speed	Sedimentation Time	TSS Removal	COD Removal
	(mg/L)	(rpm)	(min)	(%)	(%)
1	50	150	20	74.62	58.28
2	50	100	10	69.92	55.52
3	80	150	30	82.70	71.30
4	80	150	10	66.91	55.91
5	50	150	20	76.50	57.29
6	20	150	30	74.43	56.90
7	50	200	30	85.71	71.69
8	50	150	20	77.44	57.89
9	80	100	20	84.21	69.13
10	20	100	20	77.44	61.24
11	50	150	20	81.20	60.06
12	50	100	30	84.21	73.47
13	20	150	10	69.17	54.14
14	50	150	20	77.44	61.04
15	80	200	20	83.45	66.17
16	20	200	20	76.69	60.84
17	50	200	10	63.90	57.89
Control −	0	200	30	58.64	47.63
Control +	80	200	30	88.72	92.61

The experimental data, as presented in Table 5, were further analyzed using a second-order polynomial regression model, as given in Equations (1) and (2), for the responses to the decreases in TSS and COD, respectively. Both equations were then analyzed statistically using the General Linear Model (GLM) Analysis of Variance (ANOVA) test. The results of the statistical test on the response to the decrease in TSS are presented in Table 6, while the results for the response to the decrease in COD are presented in Table 7.

$$Y_1 = 77.44 + 2.44A - 0.7519B + 7.14C + 0.1880A^2 + 2.82B^2 - 4.32C^2 + 0.0000AB + 2.63AC + 1.88BC \quad (1)$$

$$Y_2 = 58.92 + 3.67A - 0.3452B + 6.24C + 0.1775A^2 + 5.26B^2 + 0.4734C^2 - 0.6411AB + 3.16AC - 1.04BC \quad (2)$$

where

Y_1: TSS removal (%);
Y_2: COD removal (%);
A: Biocoagulant concentration (mg/L);
B: Fast stirring speed (rpm);
C: Sedimentation time (min).

Table 6. ANOVA result for TSS removal.

Source	Sum of Squares	*df*	Mean Square	*F*-Value	*p*-Value	Result
Model	609.40	9	67.71	7.98	0.0061	significant
A	47.77	1	47.77	5.63	0.0495	significant
B	4.52	1	4.52	0.5327	0.4892	not significant
C	408.16	1	408.16	48.08	0.0002	significant
AB	0.0000	1	0.0000	0.0000	1.0000	not significant
AC	27.70	1	27.70	3.26	0.1138	not significant
BC	14.13	1	14.13	1.66	0.2380	not significant
A^2	0.1488	1	0.1488	0.0175	0.8984	not significant
B^2	33.47	1	33.47	3.94	0.0875	not significant
C^2	78.70	1	78.70	9.27	0.0187	significant
Residual	59.43	7	8.49			
Lack of Fit	36.46	3	12.15	2.12	0.2408	not significant
Pure Error	22.97	4	5.74			
Cor Total	668.83	16				
Fit Statistic						
R^2						0.9111
C.V. (%)						3.79

Table 7. ANOVA result for COD removal.

Source	Sum of Squares	*df*	Mean Square	*F*-Value	*p*-Value	Result
Model	585.88	9	65.10	12.62	0.0015	significant
A	107.99	1	107.99	20.93	0.0026	significant
B	0.9534	1	0.9534	0.1848	0.6802	not significant
C	311.36	1	311.36	60.35	0.0001	significant
AB	1.64	1	1.64	0.3187	0.5900	not significant
AC	39.85	1	39.85	7.72	0.0273	significant
BC	4.29	1	4.29	0.8316	0.3921	not significant
A^2	0.1327	1	0.1327	0.0257	0.8771	not significant
B^2	116.37	1	116.37	22.56	0.0021	significant
C^2	0.9438	1	0.9438	0.1829	0.6817	not significant
Residual	36.11	7	5.16			
Lack of Fit	26.20	3	8.73	3.52	0.1277	not significant
Pure Error	9.92	4	2.48			
Cor Total	621.99	16				
Fit Statistic						
R^2						0.9419
C.V.						3.68

Based on the results of statistical tests, both models showed high significance, with *p*-values of 0.0061 for the TSS removal model and 0.0015 for the COD removal model. Both values meet the 95% confidence level, as evidenced by *p*-values < 0.05, indicating that the variables and responses considered in the study are statistically significant [68,69]. As for the variables and interactions between variables that are statistically significant, namely variables A (biocoagulant concentration), C (sedimentation Time), and C^2 for the TSS removal model, and variables A (biocoagulant concentration), C (sedimentation Time),

AC, and B^2 for the COD removal model. The *F*-value test results for the TSS removal model (2.12) and the COD removal model (3.52) indicate that the lack of fit is not significant due to pure error (good fit). The coefficient of determination (R^2) values for the TSS removal model and the COD removal model are 0.9111 and 0.9419, respectively. These values indicate 91.11% agreement for the TSS and 94.19% for the COD removal models between the estimated and actual experimental results. A high R^2 value indicates that the model can be used to navigate the design space [70,71].

The graph of the relationship between variables on the TSS removal response is presented in Figure 4, while the graph for the COD removal is presented in Figure 5. The relationship graphs are presented in two-dimensional (contour) and three-dimensional graphs.

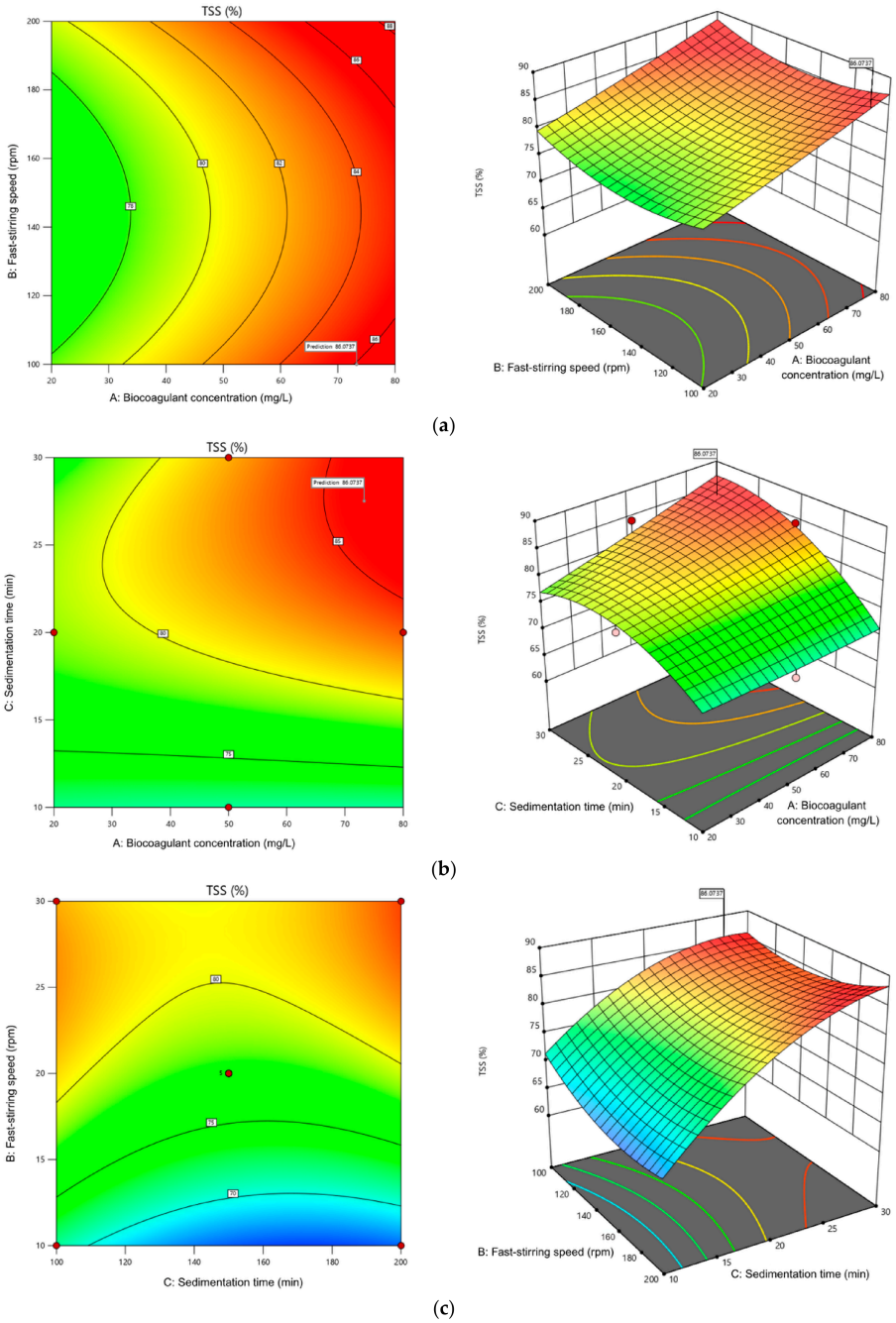

Figure 4. Interaction graph of the variables (**a**) concentration and fast stirring speed, (**b**) concentration and sedimentation time, and (**c**) fast stirring speed and sedimentation time for the response of TSS removal.

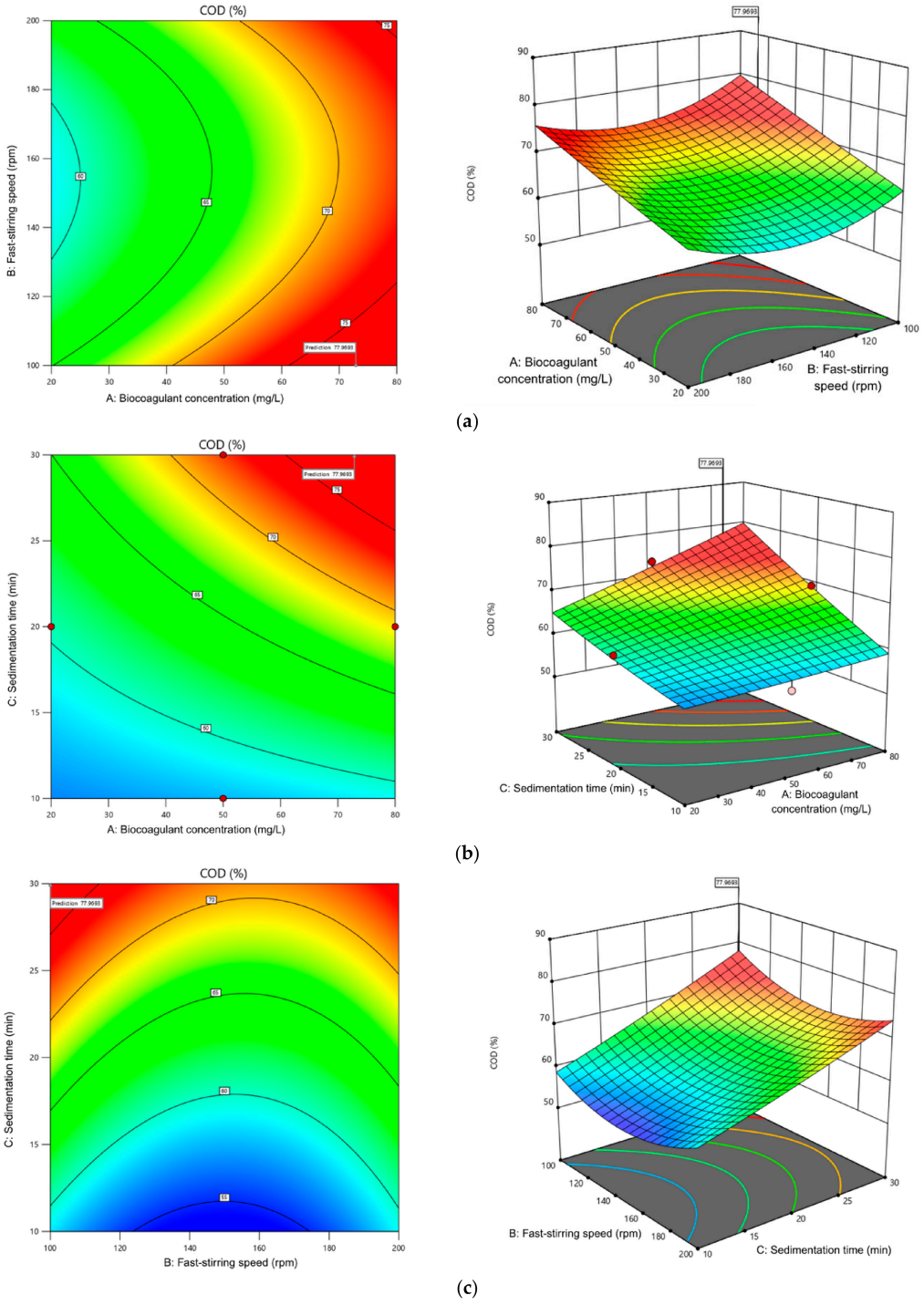

Figure 5. Interaction graph of the variables (**a**) concentration and fast stirring speed, (**b**) concentration and sedimentation time, and (**c**) fast stirring speed and sedimentation time for the response of COD removal.

Based on Figure 4a, the relationship between the concentration variable and the fast stirring speed shows a fluctuating TSS removal response and does not significantly affect it. The highest response is obtained at the highest concentration, with the lowest and highest fast stirring speeds. The response decreases in the middle range for the fast stirring speed variable. The relationship between the concentration variable and sedimentation time is shown in Figure 4b, where a significant effect is observed: the higher the concentration, the longer the sedimentation time, and the greater the TSS removal response. The relationship between the fast stirring speed variable and sedimentation time is also shown in Figure 4c, where a similar response is observed as for the concentration variable and the fast stirring

speed. The interaction of variables B (fast stirring speed) and C (sedimentation time) does not significantly affect the response. The highest TSS removal response is obtained at the longest sedimentation time and at the lowest and highest fast stirring speeds. The response decreases in the middle range of the fast stirring variable.

Figure 5a shows the relationship between the concentration variables and the fast stirring speed, which results in a fluctuating COD removal response. The interaction of variables A (biocoagulant concentration) and B (fast stirring speed) does not have a significant effect on the response. The highest response was obtained at the highest concentration, with the lowest and highest fast stirring speeds. The response decreased in the middle range for the fast stirring speed variable. The relationship between the concentration variables and sedimentation time is shown in Figure 5b, where a harmonious relationship was observed: the higher the concentration, the longer the sedimentation time, and the greater the COD removal response. The interaction of variables A (biocoagulant concentration) and C (sedimentation time) did not have a significant effect on the response. The relationship between the fast stirring speed variables and sedimentation time is also evident in Figure 5c, where a response similar to that observed between the concentration variables and the fast stirring speed is observed. The interaction of variables B (fast stirring speed) and C (sedimentation time) did not have a significant effect on the response. The highest COD removal was observed at the longest sedimentation time and at the lowest and highest fast stirring speeds. The response decreased in the middle range of the fast stirring variable. The existence of different response patterns across relationships between variables requires optimization analysis to determine the optimal point.

3.4. Optimum Condition and Validation Test

The determination of constraints is presented in Table 8. The objectives for the concentration and sedimentation time variables are set within ranges, given that both variables significantly affect TSS and COD removal responses. At the same time, the objective for the fast stirring speed variable was set to minimize it, as this variable does not significantly affect TSS and COD removal responses and tends to yield the best response at the lowest fast stirring speed. The response objective is set to the same value, namely, to maximize the response at the optimum point. The priority value (importance) is set to the same because both responses have the same position, and neither is a priority response.

Table 8. Goal constraints for optimum conditions.

Variable	Goal	Lower Limit	Upper Limit	Lower Weight	Upper Weight	Importance
A: Biocoagulant concentration	in range	20	80	1	1	1
B: Fast mixing speed	minimize	100	200	1	1	1
C: Sedimentation time	in range	10	30	1	1	1
TSS removal	maximize	63.91	85.71	1	1	3
COD removal	maximize	54.14	73.47	1	1	3

Based on these goal constraints, further analysis was conducted, and an optimal point estimate was obtained using the desirability model. The optimum conditions for the use of neem leaf biocoagulant to reduce TSS and COD levels in fisheries wastewater were: biocoagulant concentration 79.8 mg/L, fast stirring speed 100 rpm, sedimentation time 27.5 min, predicted to yield TSS removal 87.10% and COD removal 77.06% (desirability 1.00). Confirmation analysis is carried out under the optimum conditions determined by the suggested model. The results of the confirmation test for the optimum condition are presented in Table 9.

Table 9. Confirmation test results for model validation.

Model Prediction (%)		Removal in Confirmation Test (%)		Error (%)	
TSS	**COD**	**TSS**	**COD**	**TSS**	**COD**
87.10	77.06	87.97	79.98	↑ 0.99	↑ 3.66
		88.72	79.39	↑ 1.83	↑ 2.94
		88.72	77.81	↑ 1.83	↑ 0.97

↑: Increased value as compared to the model prediction

Based on the confirmation analysis, the TSS removal response confirmation rates were 87.97%, 88.72%, and 88.72%. The COD removal confirmation results were 79.98%, 79.39%, and 77.81%. These values were higher than the RSM prediction. The analysis of the error percentage calculation carried out yielded an error percentage of <5% across all confirmation test repeats for each response [72,73]. This value shows that the experimental results are consistent with the model's predictions and indicates that the model is valid [74]. Compared with previous studies, the results obtained were relatively higher. Thirugnanasambandham and Karri [20] stated that neem leaf powder removed 73% TSS and 43% COD Ahmad et al. [2] reported 82.7% removal of TSS, while Kiran and Suda [42] mentioned 63% removal of TSS.

From a practical perspective, the optimized conditions obtained in this study are compatible with conventional coagulation–flocculation processes used in aquaculture wastewater treatment. The optimum biocoagulant dosage (79.8 mg/L) is within the typical range reported for plant-based coagulants [75,76]. It is significantly lower than the dosages in the g/L range reported for some crude materials [77–79], indicating favorable chemical consumption. The fast mixing speed of 100 rpm for 1 min falls within standard design criteria for coagulation units, where fast mixing is typically applied to ensure uniform coagulant dispersion without excessive energy input. The sedimentation time of 27.5 min is also operationally feasible, as primary settling tanks in small- to medium-scale wastewater treatment systems commonly operate with detention times of 20–60 min [40,75,80]. Therefore, the proposed process does not require additional infrastructure or extended hydraulic retention time beyond conventional practice.

In terms of implementation, neem leaf powder can be prepared through simple drying and grinding steps [61], thereby supporting decentralized application in small aquaculture facilities. The biodegradability of the generated sludge represents an additional advantage over metal-based coagulants, potentially reducing sludge disposal costs [1,81]. However, large-scale applications would require evaluation of the biocoagulant's continuous-flow performance, sludge settling characteristics, storage stability, and economic feasibility, including cost–benefit and operational cost analyses. These aspects should be addressed in future pilot-scale studies. This study employed crude neem leaf powder rather than purified protein fractions. While this limits precise identification of the active coagulating molecules, the approach reflects realistic operational conditions and preserves the low-cost advantage of plant-based coagulants [61,82]. Future work should focus on fractionating protein components, determining isoelectric points, analyzing the generated sludge, correlating purified fractions with coagulation efficiency to provide a molecular-level understanding, and assessing potential trace metal release into treated water under varying operational conditions.

4. Conclusions

In conclusion, this study successfully demonstrated the efficacy of *Azadirachta indica* leaves as a biocoagulant for treating fishery wastewater, significantly reducing both total suspended solids (TSS) and chemical oxygen demand (COD). The optimized conditions de-

termined through Response Surface Methodology, specifically a biocoagulant concentration of 79.8 mg/L, fast stirring speed of 100 rpm, and sedimentation time of 27.5 min, yielded remarkable removals of 88.72% and 79.98% in TSS and COD, respectively. These findings highlight the potential of neem leaf biocoagulant as a sustainable and effective solution for managing wastewater in the fisheries sector, contributing not only to cleaner water but also to the overall health of aquatic ecosystems. As the fisheries sector continues to grow, integrating environmentally friendly treatment methods, as explored in this research, can help mitigate the negative impacts of wastewater on water bodies, thereby promoting a more sustainable approach to fisheries and environmental conservation. Future research may focus on scaling up this biocoagulation process, exploring its integration into existing wastewater treatment systems, and extracting the active protein fraction and its charge behavior as a function of pH to establish structure–activity relationships to enhance overall efficiency and effectiveness.

Author Contributions: M.F.I.: Conceptualization, funding acquisition, supervision, resources, writing—original draft, and validation; R.R.M.: Investigation, formal analysis, and writing—original draft; W.D.: Supervision and funding acquisition; E.P.K.: Supervision and funding acquisition; S.V.S.: writing—original draft; S.B.K.: Conceptualization, writing—original draft, writing—review and editing, and visualization. All authors have read and agreed to the published version of the manuscript.

Funding: This research was financially supported by the MANDAT research program from Universitas Airlangga (Grant No. 1519/UN.315/PT/2021). The APC was funded by TU Delft.

Institutional Review Board Statement: Not applicable.

Informed Consent Statement: Not applicable.

Data Availability Statement: The original contributions presented in this study are included in the article. Further inquiries can be directed to the corresponding author.

Acknowledgments: The authors also wish to thank Universiti Kebangsaan Malaysia for providing access to the analytical facilities used in this study. During the preparation of this work, the authors used ChatGPT 5.3 and Grammarly 1.156.1.0 to refine the language. After using this tool/service, the authors reviewed and edited the content as needed and they take full responsibility for the content of the publication.

Conflicts of Interest: The authors declare no conflicts of interest.

References

1. Kurniawan, S.B.; Ahmad, A.; Imron, M.F.; Abdullah, S.R.S.; Othman, A.R.; Hasan, H.A. Achieving a Biocircular Economy in the Aquaculture Sector Through Waste Valorization. *Toxics* **2025**, *13*, 131. [CrossRef]
2. Ahmad, A.; Abdullah, S.R.S.; Hasan, H.A.; Othman, A.R.; Kurniawan, S.B. Aquaculture Wastewater Treatment Using Plant-Based Coagulants: Evaluating Removal Efficiency through the Coagulation-Flocculation Process. *Results Chem.* **2024**, *7*, 101390. [CrossRef]
3. Alnawajha, M.M.; Kurniawan, S.B.; Imron, M.F.; Abdullah, S.R.S.; Hasan, H.A.; Othman, A.R. Plant-Based Coagulants/Flocculants: Characteristics, Mechanisms, and Possible Utilization in Treating Aquaculture Effluent and Benefiting from the Recovered Nutrients. *Environ. Sci. Pollut. Res.* **2022**, *29*, 58430–58453. [CrossRef]
4. Kumararaja, P.; Suvana, S.; Saraswathy, R.; Lalitha, N.; Muralidhar, M. Mitigation of Eutrophication through Phosphate Removal by Aluminium Pillared Bentonite from Aquaculture Discharge Water. *Ocean Coast. Manag.* **2019**, *182*, 104951. [CrossRef]
5. Yuliasni, R.; Kurniawan, S.B.; Marlena, B.; Hidayat, M.R.; Kadier, A.; Ma, P.C.; Imron, M.F. Recent Progress of Phytoremediation-Based Technologies for Industrial Wastewater Treatment. *J. Ecol. Eng.* **2023**, *24*, 208–220. [CrossRef]
6. Lazado, C.C.; Good, C. Survey Findings of Disinfection Strategies at Selected Norwegian and North American Land-Based RAS Facilities: A Comparative Insight. *Aquaculture* **2021**, *532*, 736038. [CrossRef]

7. Imron, M.F.; Ananta, A.R.; Ramadhani, I.S.; Kurniawan, S.B.; Abdullah, S.R.S. Potential of Lemna Minor for Removal of Methylene Blue in Aqueous Solution: Kinetics, Adsorption Mechanism, and Degradation Pathway. *Environ. Technol. Innov.* **2021**, *24*, 101921. [CrossRef]
8. Dragomir, V.D.; Dumitru, M. The State of the Research on Circular Economy in the European Union: A Bibliometric Review. *Clean. Waste Syst.* **2024**, *7*, 100127. [CrossRef]
9. Kurniawan, S.B.; Imron, M.F.; Abdullah, S.R.S.; Othman, A.R.; Hasan, H.A. Coagulation–Flocculation of Aquaculture Effluent Using Biobased Flocculant: From Artificial to Real Wastewater Optimization by Response Surface Methodology. *J. Water Process Eng.* **2023**, *53*, 103869. [CrossRef]
10. Hamidi, D.; Besharati Fard, M.; Yetilmezsoy, K.; Alavi, J.; Zarei, H. Application of Orchis Mascula Tuber Starch as a Natural Coagulant for Oily-Saline Wastewater Treatment: Modeling and Optimization by Multivariate Adaptive Regression Splines Method and Response Surface Methodology. *J. Environ. Chem. Eng.* **2021**, *9*, 104745. [CrossRef]
11. Igwegbe, C.A.; Obiora-Okafo, I.A.; Iwuozor, K.O.; Ghosh, S.; Kurniawan, S.B.; Rangabhashiyam, S.; Kanaoujiya, R.; Ighalo, J.O. Treatment Technologies for Bakers' Yeast Production Wastewater. *Environ. Sci. Pollut. Res.* **2022**, *29*, 11004–11026. [CrossRef]
12. Jamshidi, A.; Rezaei, S.; Hassani, G.; Firoozi, Z.; Ghaffari, H.R.; Sadeghi, H. Coagulating Potential of Iranian Oak (Quercus Branti) Extract as a Natural Coagulant in Turbidity Removal from Water. *J. Environ. Health Sci. Eng.* **2020**, *18*, 163–175. [CrossRef] [PubMed]
13. Noor, M.H.M.; Lee, W.J.; Mohd Azli, M.F.Z.; Ngadi, N.; Mohamed, M. Moringa Oleifera Extract as Green Coagulant for POME Treatment: Preliminary Studies and Sludge Evaluation. *Mater. Today Proc.* **2021**, *46*, 1940–1947. [CrossRef]
14. Ibrahim, M.; Ismail, N.; Chua, B.; Adnan, A. Drying And Extraction of Moringa Oleifera And Its Application In Wastewater Treatment. *J. Phys. Conf. Ser.* **2021**, *2120*, 012002. [CrossRef]
15. Mold, M.; Linhart, C.; Gómez-Ramírez, J.; Villegas-Lanau, A.; Exley, C. Aluminum and Amyloid-β in Familial Alzheimer's Disease. *J. Alzheimer's Dis.* **2020**, *73*, 1627–1635. [CrossRef]
16. Zourif, A.; Kouniba, S.; El Guendouzi, M. Valorization of Palm Petiole Waste as Natural Biocoagulants: Optimizing Coagulation-Flocculation for Sustainable Wastewater Treatment and Advancing Circular Economy in Agriculture. *Biocatal. Agric. Biotechnol.* **2025**, *63*, 103473. [CrossRef]
17. Iber, B.T.; Okomoda, V.T.; Rozaimah, S.A.; Kasan, N.A. Eco-Friendly Approaches to Aquaculture Wastewater Treatment: Assessment of Natural Coagulants Vis-a-Vis Chitosan. *Bioresour. Technol. Rep.* **2021**, *15*, 100702. [CrossRef]
18. Muda, K.; Ali, N.S.A.; Abdullah, U.N.; Sahir, A.B. Potential Use of Fruit Seeds and Plant Leaves as Coagulation Agent in Water Treatment. *J. Environ. Treat. Tech.* **2020**, *8*, 971–977.
19. Cherian, T.; Eranhottu, S.; Mohanraju, R. Process Optimization and Bioflocculative Insights of Glycoprotein Bioflocculant Produced by Marine Bacterium Bacillus Oceanisediminis LBB1. *Biocatal. Agric. Biotechnol.* **2025**, *65*, 103555. [CrossRef]
20. Thirugnanasambandham, K.; Karri, R.R. Preparation and Characterization of Azadirachta Indica A. Juss. Plant Based Natural Coagulant for the Application of Urban Sewage Treatment: Modelling and Cost Assessment. *Environ. Technol. Innov.* **2021**, *23*, 101733. [CrossRef]
21. Priyatharishini, M.; Mokhtar, N.M.M. Performance of Jackfruit (*Artocarpus heterophyllus*) Peel Coagulant in Turbidity Reduction under Different PH of Wastewater. *Mater. Today Proc.* **2021**, *46*, 1818–1823. [CrossRef]
22. Daverey, A.; Tiwari, N.; Dutta, K. Utilization of Extracts of Musa Paradisica (Banana) Peels and Dolichos Lablab (Indian Bean) Seeds as Low-Cost Natural Coagulants for Turbidity Removal from Water. *Environ. Sci. Pollut. Res.* **2019**, *26*, 34177–34183. [CrossRef]
23. Vasanthy, M.; Ravindran, B.; Chung, W.J.; Chang, S.W. Treatment of Coffee Cherry Pulping Wastewater by Using Lectin Protein Isolated from *Ricinus communis* L. Seed. *J. Water Process Eng.* **2021**, *39*, 101742. [CrossRef]
24. Rifi, S.K.; Souabi, S.; El Fels, L.; Driouich, A.; Nassri, I.; Haddaji, C.; Hafidi, M. Optimization of Coagulation Process for Treatment of Olive Oil Mill Wastewater Using Moringa Oleifera as a Natural Coagulant, CCD Combined with RSM for Treatment Optimization. *Process Saf. Environ. Prot.* **2022**, *162*, 406–418. [CrossRef]
25. Muralimohan, D.N.; Augustin, S.; Meiyazhagan, G.; Sethupathi, P.; Ramesh, V. An Experimental Investigation on Treatment of Tannery Effluent Using Azadirachta Indica. *Int. J. Environ. Agric. Biotechnol.* **2017**, *2*, 762–766. [CrossRef]
26. Ahmad, A.; Abdullah, S.R.S.; Hasan, H.A.; Othman, A.R.; Ismail, N.I. Plant-Based versus Metal-Based Coagulants in Aquaculture Wastewater Treatment: Effect of Mass Ratio and Settling Time. *J. Water Process Eng.* **2021**, *43*, 102269. [CrossRef]
27. Fard, M.B.; Hamidi, D.; Yetilmezsoy, K.; Alavi, J.; Hosseinpour, F. Utilization of Alyssum Mucilage as a Natural Coagulant in Oily-Saline Wastewater Treatment. *J. Water Process Eng.* **2021**, *40*, 101763. [CrossRef]
28. Amran, A.H.; Zaidi, N.S.; Syafiuddin, A.; Zhan, L.Z.; Bahrodin, M.B.; Mehmood, M.A.; Boopathy, R. Potential of Carica Papaya Seed-Derived Bio-Coagulant to Remove Turbidity from Polluted Water Assessed through Experimental and Modeling-Based Study. *Appl. Sci.* **2021**, *11*, 5715. [CrossRef]

29. Daud, N.M.; Sheikh Abdullah, S.R.; Abu Hasan, H. Response Surface Methodological Analysis for the Optimization of Acid-Catalyzed Transesterification Biodiesel Wastewater Pre-Treatment Using Coagulation–Flocculation Process. *Process Saf. Environ. Prot.* **2018**, *113*, 184–192. [CrossRef]
30. Ezemagu, I.G.; Ejimofor, M.I.; Menkiti, M.C.; Nwobi-Okoye, C.C. Modeling and Optimization of Turbidity Removal from Produced Water Using Response Surface Methodology and Artificial Neural Network. *S. Afr. J. Chem. Eng.* **2021**, *35*, 78–88. [CrossRef]
31. *6989.59:2008*; Air dan air limbah—Bagian 59: Metoda pengambilan contoh air limbah. Badan Standarisasi Nasional: Jakarta, Indonesia, 2008.
32. Kalibbala, H.M.; Olupot, P.W.; Ambani, O.M. Synthesis and Efficacy of Cactus-Banana Peels Composite as a Natural Coagulant for Water Treatment. *Results Eng.* **2023**, *17*, 100945. [CrossRef]
33. Othmani, B.; Rasteiro, M.G.; Khadhraoui, M. Toward Green Technology: A Review on Some Efficient Model Plant-Based Coagulants/Flocculants for Freshwater and Wastewater Remediation. *Clean Technol. Environ. Policy* **2020**, *22*, 1025–1040. [CrossRef]
34. Igwegbe, C.A.; Onukwuli, O.D. Removal of Total Dissolved Solids (TDS) from Aquaculture Wastewater by Coagulation-Flocculation Process Using Sesamum Indicum Extract: Effect of Operating Parameters and Coagulation-Flocculation Kinetics. *Pharm. Chem. J.* **2019**, *6*, 32–45.
35. Berent, K.; Komarek, S.; Lach, R.; Pyda, W. The Effect of Calcination Temperature on the Structure and Performance of Nanocrystalline Mayenite Powders. *Materials* **2019**, *12*, 3476. [CrossRef]
36. Othman, A.R.; Ismail, N.S.; Abdullah, S.R.S.; Hasan, H.A.; Kurniawan, S.B.; Sharuddin, S.S.N.; Ismail, N. Izzati Potential of Indigenous Biosurfactant-Producing Fungi from Real Crude Oil Sludge in Total Petroleum Hydrocarbon Degradation and Its Future Research Prospects. *J. Environ. Chem. Eng.* **2022**, *10*, 107621. [CrossRef]
37. Nakhaei Pour, A.; Mohammadi, A. Effects of Synthesis Parameters on Organic Template-Free Preparation of Zeolite Y. *J. Inorg. Organomet. Polym. Mater.* **2021**, *31*, 2501–2510. [CrossRef]
38. Ali, A.; Chiang, Y.W.; Santos, R.M. X-Ray Diffraction Techniques for Mineral Characterization: A Review for Engineers of the Fundamentals, Applications, and Research Directions. *Minerals* **2022**, *12*, 205. [CrossRef]
39. Kurniawan, S.B.; Imron, M.F.; Abdullah, S.R.S.; Othman, A.R.; Purwanti, I.F.; Hasan, H.A. Treatment of Real Aquaculture Effluent Using Bacteria-Based Bioflocculant Produced by Serratia Marcescens. *J. Water Process Eng.* **2022**, *47*, 102708. [CrossRef]
40. Miyashiro, C.S.; Mateus, G.A.P.; dos Santos, T.R.T.; Paludo, M.P.; Bergamasco, R.; Fagundes-Klen, M.R. Synthesis and Performance Evaluation of a Magnetic Biocoagulant in the Removal of Reactive Black 5 Dye in Aqueous Medium. *Mater. Sci. Eng. C* **2021**, *119*, 111523. [CrossRef]
41. *SNI 19-6449-2000*; Metode Pengujian Koagulasi—Flokulasi dengan Cara Jar. Badan Standarisasi Nasional: Jakarta, Indonesia, 2000.
42. Soumya Kiran, P.; Reddy Suda, V.B.B. Reduction of Turbidity by Adding Bio Coagulant-A Sustainable Approach. In *IOP Conference Series: Earth and Environmental Science*; IOP Publishing: Bristol, UK, 2022; Volume 982, p. 012039. [CrossRef]
43. Venegas-García, D.J.; Wilson, L.D. Utilization of Bioflocculants from Flaxseed Gum and Fenugreek Gum for the Removal of Arsenicals from Water. *Materials* **2022**, *15*, 8691. [CrossRef] [PubMed]
44. Peng, Y.; Khaled, U.; Al-Rashed, A.A.A.A.; Meer, R.; Goodarzi, M.; Sarafraz, M.M. Potential Application of Response Surface Methodology (RSM) for the Prediction and Optimization of Thermal Conductivity of Aqueous CuO (II) Nanofluid: A Statistical Approach and Experimental Validation. *Phys. A Stat. Mech. Its Appl.* **2020**, *554*, 124353. [CrossRef]
45. Chua, S.-C.; Chong, F.-K.; Malek, M.A.; Ul Mustafa, M.R.; Ismail, N.; Sujarwo, W.; Lim, J.-W.; Ho, Y.-C. Optimized Use of Ferric Chloride and Sesbania Seed Gum (SSG) as Sustainable Coagulant Aid for Turbidity Reduction in Drinking Water Treatment. *Sustainability* **2020**, *12*, 2273. [CrossRef]
46. Standard Methods Committee of the American Public Health Association, American Water Works Association, and Water Environment Federation. 2540 solids. In *Standard Methods For the Examination of Water and Wastewater*; APHA Press: Washington, DC, USA, 2023. [CrossRef]
47. Standard Methods Committee of the American Public Health Association, American Water Works Association, and Water Environment Federation. 5220 chemical oxygen demand (cod). In *Standard Methods For the Examination of Water and Wastewater*; Lipps, W.C., Baxter, T.E., Braun-Howland, E., Eds.; APHA Press: Washington, DC, USA, 2023. [CrossRef]
48. Iber, B.T.; Kasan, N.A. Recent Advances in Shrimp Aquaculture Wastewater Management. *Heliyon* **2021**, *7*, e08283. [CrossRef] [PubMed]
49. Brod, E.; Øgaard, A.F. Closing Global P Cycles: The Effect of Dewatered Fish Sludge and Manure Solids as P Fertiliser. *Waste Manag.* **2021**, *135*, 190–198. [CrossRef]
50. Kar, S.; Sangem, P.; Anusha, N.; Senthilkumaran, B. Endocrine Disruptors in Teleosts: Evaluating Environmental Risks and Biomarkers. *Aquac. Fish.* **2021**, *6*, 1–26. [CrossRef]

51. Ezziddine, M.; Liltved, H.; Homme, J.M. A Method for Reclaiming Nutrients from Aquacultural Waste for Use in Soilless Growth Systems. *Water Sci. Technol.* **2020**, *81*, 81–90. [CrossRef]
52. Hussain, G.; Haydar, S. Exploring Potential of Pearl Millet (*Pennisetum glaucum*) and Black-Eyed Pea (*Vigna unguiculata* subsp. unguiculata) as Bio-Coagulants for Water Treatment. *Desalin. Water Treat.* **2019**, *143*, 184–191. [CrossRef]
53. Kumar, R.; Sharma, S.; Devi, L. Investigation of Total Phenolic, Flavonoid Contents and Antioxidant Activity from Extracts of Azadirachta Indica of Bundelkhand Region. *Int. J. Life-Sci. Sci. Res.* **2018**, *4*, 1925–1933. [CrossRef]
54. Oyekanmi, A.A.; Kumar, U.S.U.; Abdul Khalil, H.P.S.; Olaiya, N.G.; Amirul, A.A.; Rahman, A.A.; Nuryawan, A.; Abdullah, C.K.; Rizal, S. Functional Properties of Antimicrobial Neem Leaves Extract Based Macroalgae Biofilms for Potential Use as Active Dry Packaging Applications. *Polymers* **2021**, *13*, 1664. [CrossRef]
55. Zambri, N.D.S.; Taib, N.I.; Latif, F.A.; Mohamed, Z. Utilization of Neem Leaf Extract on Biosynthesis of Iron Oxide Nanoparticles. *Molecules* **2019**, *24*, 3803. [CrossRef]
56. Tulashie, S.K.; Adjei, F.; Abraham, J.; Addo, E. Potential of Neem Extracts as Natural Insecticide against Fall Armyworm (*Spodoptera frugiperda* (J. E. Smith) (Lepidoptera: Noctuidae). *Case Stud. Chem. Environ. Eng.* **2021**, *4*, 100130. [CrossRef]
57. Kurniawan, S.B.; Abdullah, S.R.S.; Othman, A.R.; Purwanti, I.F.; Imron, M.F.; Ismail, N.I.; Ahmad, A.; Hasan, H.A. Isolation and Characterisation of Bioflocculant-Producing Bacteria from Aquaculture Effluent and Its Performance in Treating High Turbid Water. *J. Water Process Eng.* **2021**, *42*, 102194. [CrossRef]
58. Crab, R.; Defoirdt, T.; Bossier, P.; Verstraete, W. Biofloc Technology in Aquaculture: Beneficial Effects and Future Challenges. *Aquaculture* **2012**, *356–357*, 351–356. [CrossRef]
59. Montenegro-Landívar, M.F.; Tapia-Quirós, P.; Vecino, X.; Reig, M.; Valderrama, C.; Granados, M.; Cortina, J.L.; Saurina, J. Fruit and Vegetable Processing Wastes as Natural Sources of Antioxidant-Rich Extracts: Evaluation of Advanced Extraction Technologies by Surface Response Methodology. *J. Environ. Chem. Eng.* **2021**, *9*, 105330. [CrossRef]
60. Alnawajha, M.M.; Abdullah, S.R.S.; Hasan, H.A.; Othman, A.R.; Kurniawan, S.B. Effectiveness of Using Water-Extracted Leucaena Leucocephala Seeds as a Coagulant for Turbid Water Treatment: Effects of Dosage, PH, Mixing Speed, Mixing Time, and Settling Time. *Biomass Convers. Biorefinery* **2024**, *14*, 11203–11216. [CrossRef]
61. Kurniawan, S.B.; Ahmad, A.; Said, N.S.M.; Gustinasari, K.; Abdullah, S.R.S.; Imron, M.F. The Influence of Preparation and Pretreatment on the Physicochemical Properties and Performance of Plant-Based Biocoagulants in Treating Wastewater. *Environ. Adv.* **2023**, *14*, 100441. [CrossRef]
62. Devi, G.; Alkalbani, M.S.; Jesil, A.; Dumaran, J.J.C.; Buscano, S.I. Removal of Organic Pollutants from Textile Mill Effluent Using Azadirachta Indica Powder. *Trends Sci.* **2021**, *18*, 1412. [CrossRef]
63. Kristianto, H.; Paulina, S.; Muliarahayu Soetedjo, J.N. Exploration of Various Indonesian Indigenous Plants as Natural Coagulants for Synthetic Turbid Water. *Int. J. Technol.* **2018**, *9*, 464–471. [CrossRef]
64. Al-Alawy, A.F.H.; Al-Naemi, A.N.A.; Hussein, M.Y. Zeta Potential, Effective Membrane Charge and Donnan Potential for TiO2 NF Ceramic Membrane. *J. Eng.* **2018**, *24*, 21–40. [CrossRef]
65. Hasan, H.A.; Ezril Hafiz, R.; Muhamad, M.H.; Sheikh Abdullah, S.R.; Hasan, H.A.; Ezril Hafiz, R.; Muhamad, M.H.; Sheikh Abdullah, S.R.; Hassimi, A.H.; Ezril Hafiz, R.; et al. Bioflocculant Production Using Palm Oil Mill and Sago Mill Effluent as a Fermentation Feedstock: Characterization and Mechanism of Flocculation. *J. Environ. Manag.* **2020**, *260*, 110046. [CrossRef]
66. Lapointe, M.; Barbeau, B. Understanding the Roles and Characterizing the Intrinsic Properties of Synthetic vs. Natural Polymers to Improve Clarification through Interparticle Bridging: A Review. *Sep. Purif. Technol.* **2020**, *231*, 115893. [CrossRef]
67. Kakoi, B.; Kaluli, J.W.; Ndiba, P.; Thiong'o, G. Banana Pith as a Natural Coagulant for Polluted River Water. *Ecol. Eng.* **2016**, *95*, 699–705. [CrossRef]
68. Subari, F.; Kamaruzzaman, M.A.; Abdullah, S.R.S.; Hasan, H.A.; Othman, A.R. Simultaneous Removal of Ammonium and Manganese in Slow Sand Biofilter (SSB) by Naturally Grown Bacteria from Lake Water and Its Diverse Microbial Community. *J. Environ. Chem. Eng.* **2018**, *6*, 6351–6358. [CrossRef]
69. Kiridi, E.A.; Ogunlela, A.O. Phytoremediation Rates of Morning Glory (*Ipomea asarifolia*) in an Aquaculture Effluent Hydroponic System. In *IOP Conference Series: Earth and Environmental Science*; IOP Publishing: Bristol, UK, 2020; Volume 445, p. 012020. [CrossRef]
70. David, I.J.; Adubisi, O.D.; Ogbaji, O.E.; Eghwerido, J.T.; Umar, Z.A. Resistant Measures in Assessing the Adequacy of Regression Models. *Sci. Afr.* **2020**, *8*, e00437. [CrossRef]
71. Chong, D.J.S.; Chan, Y.J.; Arumugasamy, S.K.; Yazdi, S.K.; Lim, J.W. Optimisation and Performance Evaluation of Response Surface Methodology (RSM), Artificial Neural Network (ANN) and Adaptive Neuro-Fuzzy Inference System (ANFIS) in the Prediction of Biogas Production from Palm Oil Mill Effluent (POME). *Energy* **2023**, *266*, 126449. [CrossRef]
72. Said, F.M.; Gan, J.Y.; Sulaiman, J. Correlation between Response Surface Methodology and Artificial Neural Network in the Prediction of Bioactive Compounds of Unripe Musa Acuminata Peel. *Eng. Sci. Technol. Int. J.* **2020**, *23*, 781–787. [CrossRef]

73. Bala, N.; Napiah, M.; Kamaruddin, I.; Danlami, N. Optimization of Nanocomposite Modified Asphalt Mixtures Fatigue Life Using Response Surface Methodology. In *IOP Conference Series: Earth and Environmental Science*; IOP Publishing: Bristol, UK, 2018; Volume 140. [CrossRef]
74. Nurus, M.; Nurdiawa, O.; Martanto, M. Analisis Jaringan Akses Fiber to The Home Menggunakan Teknologi Gigabit Passive Optical Network. *J. Janitra Inform. Dan Sist. Inf.* **2023**, *3*, 56–66. [CrossRef]
75. Sher, F.; Hanif, K.; Rafey, A.; Khalid, U.; Zafar, A.; Ameen, M.; Lima, E.C. Removal of Micropollutants from Municipal Wastewater Using Different Types of Activated Carbons. *J. Environ. Manag.* **2021**, *278*, 111302. [CrossRef]
76. Gandiwa, B.I.; Moyo, L.B.; Ncube, S.; Mamvura, T.A.; Mguni, L.L.; Hlabangana, N. Optimisation of Using a Blend of Plant Based Natural and Synthetic Coagulants for Water Treatment: (Moringa Oleifera-Cactus Opuntia-Alum Blend). *S. Afr. J. Chem. Eng.* **2020**, *34*, 158–164. [CrossRef]
77. Teh, C.Y.; Wu, T.Y.; Juan, J.C. Potential Use of Rice Starch in Coagulation-Flocculation Process of Agro-Industrial Wastewater: Treatment Performance and Flocs Characterization. *Ecol. Eng.* **2014**, *71*, 509–519. [CrossRef]
78. Saritha, V.; Srinivas, N.; Srikanth Vuppala, N.V. Analysis and Optimization of Coagulation and Flocculation Process. *Appl. Water Sci.* **2017**, *7*, 451–460. [CrossRef]
79. Ahmad, A.; Abdullah, S.R.S.; Hasan, H.A.; Othman, A.R.; Ismail, N. Izzati Potential of Local Plant Leaves as Natural Coagulant for Turbidity Removal. *Environ. Sci. Pollut. Res.* **2021**, *29*, 2579–2587. [CrossRef]
80. Heiderscheidt, E.; Tesfamariam, A.; Pulkkinen, J.; Vielma, J.; Ronkanen, A.K. Solids Management in Freshwater-Recirculating Aquaculture Systems: Effectivity of Inorganic and Organic Coagulants and the Impact of Operating Parameters. *Sci. Total Environ.* **2020**, *742*, 140398. [CrossRef]
81. Chakraborty, T.; Balusani, D.; Smith, S.; Santoro, D.; Walton, J.; Nakhla, G.; Ray, M.B. Reusability of Recovered Iron Coagulant from Primary Municipal Sludge and Its Impact on Chemically Enhanced Primary Treatment. *Sep. Purif. Technol.* **2020**, *231*, 115894. [CrossRef]
82. Nnaji, P.C.; Anadebe, V.C.; Ezemagu, I.G.; Onukwuli, O.D. Potential of Luffa Cylindrica Seed as Coagulation-Flocculation (CF) Agent for the Treatment of Dye Wastewater: Kinetic, Mass Transfer, Optimization and CF Adsorption Studies. *Arab. J. Chem.* **2022**, *15*, 103629. [CrossRef]